

## Article

# Mesityl Oxide Reduction by Using Acid-Modified Phonolite Supported NiW, NiMo, and CoMo Catalysts

José Miguel Hidalgo Herrador <sup>\*</sup>, Zdeněk Tišler , Jaroslav Kocík, Jakub Frańczak, Ivana Hradecká, Romana Velvarská and Héctor de Paz Carmona 

ORLEN UniCRE a.s., Revoluční 1521/84, 400 01 Ústí nad Labem, Czech Republic; zdenek.tisler@orlenuicre.cz (Z.T.); jaroslav.kocik@orlenuicre.cz (J.K.); jakub.franczak@orlenuicre.cz (J.F.); ivana.hradecka@orlenuicre.cz (I.H.); romana.velvarska@orlenuicre.cz (R.V.); hector.carmona@orlenuicre.cz (H.d.P.C.)

\* Correspondence: jose.hidalgo@orlenuicre.cz; Tel.: +420-731-534-973

**Abstract:** Mesityl oxide is standardly used to produce methyl iso butyl ketone but it can be also used to produce other useful compounds. Three catalysts were used for the reaction of the mesityl oxide reduction. They were NiW, NiMo, and CoMo supported on phonolite modified by HCl (metals/Ph-HCl). The fresh catalysts were characterized by XRD, XRF, BET surface, Hg porosimetry, SEM, H<sub>2</sub>-TPR, NH<sub>3</sub>-TPD, CO<sub>2</sub>-TPD. The materials were directly used, previously reduced in H<sub>2</sub> or sulfided for the mesityl oxide reduction under H<sub>2</sub> atmosphere. The reaction was performed in an autoclave at T = 375 °C, p = 50 bar (H<sub>2</sub>), and TOS = 1.5 h. The products were analyzed by GC/MS, GC/FID-TCD, ATR. The main products were methyl isobutyl ketone, 2-methyl pentane, and 2-methyl-2-pentene. Sulfided metal catalysts were the most active in the methyl isobutyl ketone, where the NiWSx/Ph-HCl catalyst showed the highest activity. For the non-previously-activated and hydrogen activated catalysts the most active catalyst was the NiMo/Ph-HCl for the production of methyl isobutyl ketone. The catalyst CoMo/Ph-HCl activated in hydrogen was the most active for the production of 2-methyl pentane compared to the other two hydrogen-activated materials.

**Keywords:** mesityl oxide; methyl isobutyl ketone; phonolite; catalyst; reduction; autoclave; hydrotreatment



**Citation:** Hidalgo Herrador, J.M.; Tišler, Z.; Kocík, J.; Frańczak, J.; Hradecká, I.; Velvarská, R.; de Paz Carmona, H. Mesityl Oxide Reduction by Using Acid-Modified Phonolite Supported NiW, NiMo, and CoMo Catalysts. *Catalysts* **2021**, *11*, 1101. <https://doi.org/10.3390/catal11091101>

Academic Editor: Sónia Carabineiro

Received: 13 August 2021

Accepted: 11 September 2021

Published: 13 September 2021

**Publisher's Note:** MDPI stays neutral with regard to jurisdictional claims in published maps and institutional affiliations.



**Copyright:** © 2021 by the authors. Licensee MDPI, Basel, Switzerland. This article is an open access article distributed under the terms and conditions of the Creative Commons Attribution (CC BY) license (<https://creativecommons.org/licenses/by/4.0/>).

## 1. Introduction

Mesityl oxide (MSO) can be obtained from acetone by aldol condensation reaction producing diacetone alcohol (DAA). MSO can be used as solvent for phenol-formaldehyde resins, in PVC compounds and urea derivatives as feed for cattle, sheep, and poultry [1]. In addition, it can be also used in general as a solvent for synthetic fibers and rubbers, oils, gums, resins, lacquers, varnishes, inks, stains, and insect repellent [2].

Then, the dehydration of this compound produces MSO [3,4]. MSO can be used as a solvent or an intermedium product to produce methyl isobutyl ketone (MIBK). On a commercial scale, acetone is produced by the cumene hydroperoxide process. Nevertheless, it can also be produced by dehydrogenation of 2-propanol (isopropyl alcohol) [3–5].

Concretely, the significance of MSO reduction in the area of catalyst research is an important topic because other important products can be produced from it taking also into account its availability in the industry [1,2]. The MSO is the 4-methyl-3-pentene-2-one and this molecule is an attractive molecule from the basic and applied research point of view because of the possibility of effecting reaction at the double bond, the carbonyl group, the -methyl group, or simultaneously some of these sites [3–7]. From the basic research point of view, the reduction of MSO led to the catalytic hydrogenation of a  $\beta$ -unsaturated ketone model molecule and it constitutes interesting kinetic research of selectivity and activity. Theoretically and already experimentally proven, the MSO can produce saturated ketone, unsaturated alcohol or hydrocarbon. The reduction proceeds

through the saturated carbonyl group [3–7]. From the applied research point of view, the use of MSO as raw material for different reactions is not a new process, and the mechanisms of reaction have been already studied [6,7]. However, the research on this compound is continuing nowadays because it is the precursor of the MIBK. The reaction of the MSO reduction produced MIBK and methyl isobutyl carbinol (MIBC) [7] directly. However, the hydrogenolysis of the MSO, as published by Wisniak et al. [7], can produce 2-methyl pentane (2MP) by removing the carbonyl group. O’Keefe et al. [8] published a more detailed reaction mechanism for the MSO reactions, but they did not include hydrocarbons production. Many types of catalysts have been used for the MSO reaction. Researchers have used mainly noble metal-based catalysts [8,9] using the raw material of acetone directly to produce MIBK [9–11]. However, sulfided metal catalysts are not exposed in the same detail and amount as noble metal-based materials. An example was mentioned by Houser et al. [6], in which the catalyst used was a  $WS_2-(NH_4)_2WS_4$  material. However, no details were given by the authors of that work [6]. Another reference relative to the use of metal sulfide catalysts for the total hydrogenation of the carbonyl group to methyl or methylene group was found in the book published by Weisser et al. [12]. In this case, catalysts using  $MoS_2$  and  $WS_2$  were used, obtaining 80 to 90% yields of the respective hydrocarbons at temperatures of 300–330 °C and initial hydrogen pressures at 20 °C of 100–130 atm [12]. So, new information about the mesityl oxide reduction using sulfide metal catalysts will improve the knowledge about this type of reaction.

Regarding the most common products from MSO, such as the MIBK, it can be obtained with pressures ranging from 10 to 100 bar and temperatures from 120 to 160 °C using Pd on different acid-base supports  $CaO-MgO-SrO-Al_2O_3$ ,  $ZrO(OH)_2$ -carbon,  $Nb_2O_5/SiO_2$ , or a cation exchange resin. Acetone conversions ranging from 30 to 50% were obtained with high MIBK selectivity (>90%) [6–11]. For the 2MP, which could be used as gasoline fuel, Pt on zeolite catalyst was used in the case of the MIBK hydrogenation to 2MP [11], indicating the little data available in this concrete reaction. However, the 2MP production regarding the MIBK production, as a cost-effective process, will depend on the market needs.

Metal sulfided supported catalysts are commonly used in refinery. In addition, if these catalysts can be synthesized and the raw materials for their synthesis can be found nearby (for example the support could be a mineral source near to the refinery), the probability of improving the final costs of the overall process for the obtaining of chemicals or fuels (from MSO in this case) increases a lot.

In this work, the aim was to gain more knowledge about the MSO reduction by using metal sulfide catalysts. In addition, we used a catalyst based on the modification of a mineral source of phonolite (Ph) which is located near to the refinery in the Northwest of Czech Republic with the aim of obtaining a cost-effective catalyst similar to the commercial metal sulfide catalysts based on the use of a support with high contents of  $SiO_2-Al_2O_3$  [13–15]. A previous experience by using a NiW-supported catalyst on oxalic acid modified Ph for the production of MIBK led to continue with the research of the MSO reduction [16]. Three catalysts based on NiW, NiMo, CoMo supported on acid modified Ph [17] were tested in the MSO reduction giving as main products the MIBK, 2MP, and 2-methyl-2-pentene (MPe).

## 2. Results and Discussion

### 2.1. Catalysts Characterization

X-ray fluorescence (XRF) was performed to determine the elemental composition of the fresh materials (Table 1). As previously published, the phonolite treatment with acids (HCl and oxalic acid) led to a reduction in the Al, Na, Fe, and Ca contents. The results for Ni and W contents (impregnated materials) were as expected, with the NiW/Ph-HCl. However, the Mo content in the catalysts with NiMo and CoMo was much higher than expected using a similar method of impregnation compared to the impregnation of Ni and W. The acid treatments led to a higher porosity, with the support being the most porous material (Ph-HCl).

**Table 1.** X-ray fluorescence (XRF) elemental analysis for the supports, original Ph material, and catalysts. Textural properties of the original Ph material and its derived solids.

	Ph <sup>1</sup>	Ph-HCl <sup>1</sup>	NiW/Ph-HCl <sup>1</sup>	NiMo/Ph-HCl <sup>2</sup>	CoMo/Ph-HCl
Si, wt%	26.5	34.8	28.5	28.9	29.6
Al, wt%	11.8	6.7	5.3	5.5	5.7
Ni, wt%	0.0	0.0	5.2	5.4	0.0
W, wt%	0.0	0.0	9.8	0.0	0.0
Mo, wt%	0.0	0.0	0.0	10.0	9.0
Co, wt%	0.0	0.0	0.0	0.0	4.6
Na, wt%	7.9	2.8	1.7	1.2	1.4
K, wt%	5.1	6.6	5.2	2.8	2.7
Fe, wt%	1.4	0.8	0.5	0.6	0.6
Ca, wt%	0.7	0.0	0.0	0.1	0.1
Ti, wt%	0.2	0.0	0.0	0.1	0.1
Cl, wt%	0.3	0.0	0.0	0.0	0.0
Others, wt%	0.0	<0.1	0.5	0.0	0.0
O <sup>3</sup> , wt%	46.1	48.3	43.3	45.4	46.2
* Total Intrusion Volume, cm <sup>-3</sup> g <sup>-1</sup>	0.008	0.179	0.118	0.200	0.209
* Pore volume 3–50 nm (cm <sup>3</sup> g <sup>-1</sup> )	0.003	0.030	0.016	0	0
** BET surface Area, m <sup>2</sup> g <sup>-1</sup>	7.6	120.1	53.9	41.8	51.3

<sup>1</sup> Materials used for a previous work too [14]. <sup>2</sup> Catalyst used in a previous work too [18]. <sup>3</sup> Oxygen content calculated by weight difference.

\* Hg porosimetry. \*\* N<sub>2</sub> physisorption.

The total porosity for metal oxide-supported solids prepared on the basis of these modified phonolite supports were all lower in value (Table 1), which is related to the blocking of the pores by the deposited metals (Ni, W, Mo, and Co).

The contents of Ni and W for NiW/Ph-HCl material were 5.2 and 9.8 wt%, the contents of Ni and Mo for NiMo/Ph-HCl 7.7 and 23.6 wt%, and finally the contents of Co and Mo for CoMo/Ph-HCl were 9.1 and 23.6 wt% (Table 1). In addition, significant contents of K, Na, and Fe were found for the catalysts. Concretely, 6.6, 5.2, and 4.2 wt% of K, 1.7, 1.1, and 0.9 wt% of Na, and 0.5, 0.5, and 0.4 wt% of Fe for NiW/Ph-HCl, NiMo/Ph-HCl, and CoMo/Ph-HCl materials respectively.

X-ray diffraction (XRD) analysis was performed to obtain information about the catalyst structures. The XRD diagrams (Figure 1) were similar for all solids (i.e., the signals had the same angle). However, the XRD patterns for the Ph-HCl material showed more intense signals related to the feldspar group minerals (sanidine, analcime, and nepheline) [19]. In the case of the materials containing Ni, no clear evidence of NiO crystal phase was found. There was no evidence of NiO crystal phase for the solids containing Ni at 2θ about 38 (111), 43 (200), and 62.5 (220) [20]. The reflections associated with WO<sub>3</sub> (220) were not clear (NiW/Ph-HCl catalyst) [21]. No cobalt oxide XRD patterns were found [22].

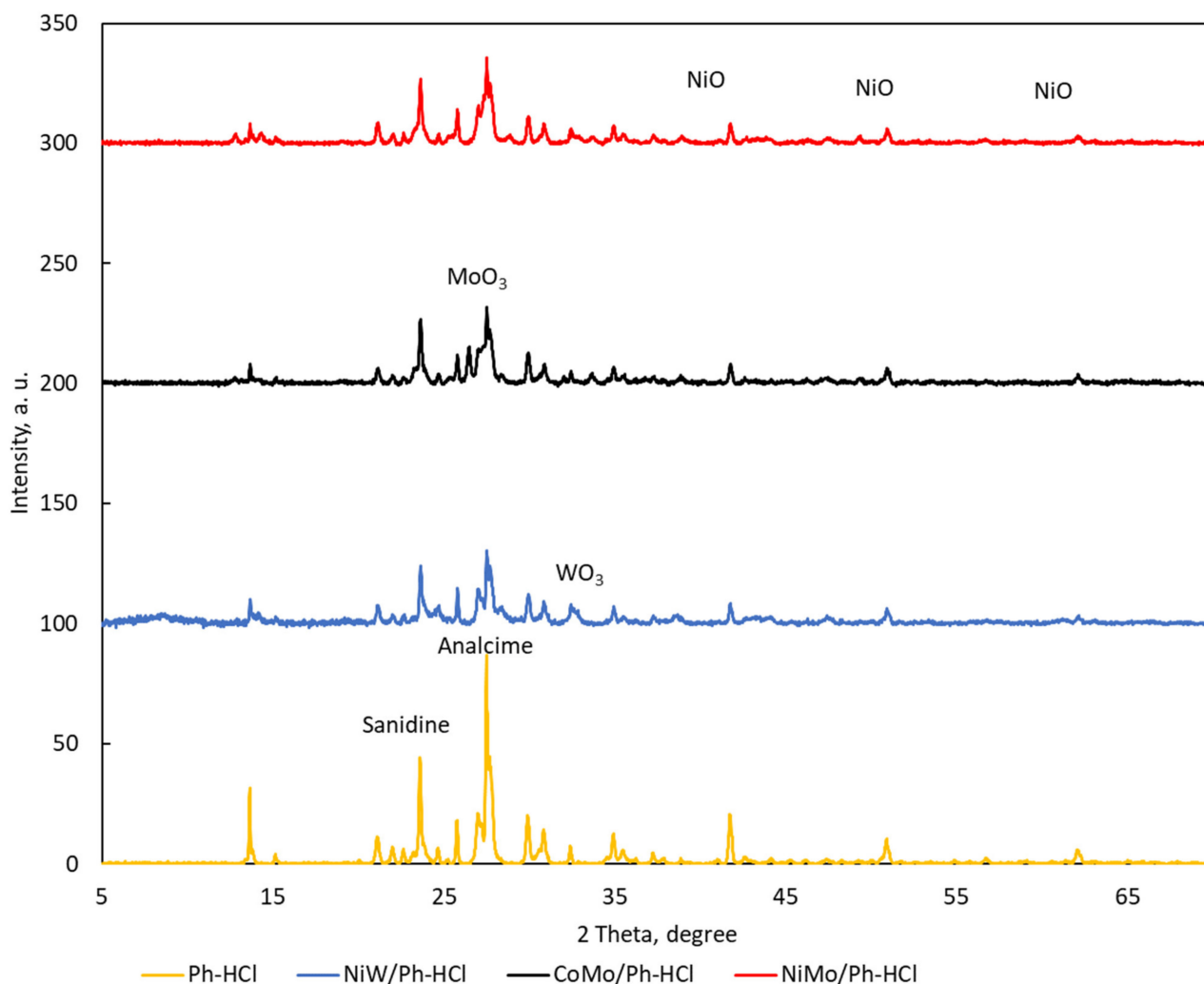


**Figure 1.** Wide angle X-ray diffraction (XRD) patterns of the Ph solids.

Hydrogen temperature-programmed reduction ( $H_2$ -TPR) patterns are shown in Figure 2. Two reduction peaks (signal maximum at 363 and 593 °C due to the nickel and tungsten oxides reduction) were observed for NiW/Ph-HCl catalyst. For NiMo catalysts, the maximum at 500 °C is due to the reduction of  $Mo^{6+}$  to  $Mo^{4+}$  of polymeric octahedral Mo species and  $NiMoO_4^{2-}$ -like phase [23]. The reduction peak at about 730 °C could be produced by reducing tetrahedrally coordinated Mo species ( $MoO_3$  phase) [23].

The CoMo/Ph-HCl  $H_2$ -TPR profiles are shown in Figure 2. It exhibits primarily two peaks reduction pattern, with the maxima centered at approximately 300 °C, which can be assigned to the reduction of  $Co_3O_4$  to CoO and then the further reduction of CoO to metallic Co (about 500 °C) [24].

Ammonia temperature-programmed desorption ( $NH_3$ -TPD) characterization was performed to study the acidity of the supports before being impregnated (Figure 3). All metal oxide supported materials presented the main zone of desorption peaks (50–250 °C) corresponding to the zone of weak and intermediate acid sites. The maximum of all the signals was found in the range of 100–110 °C.

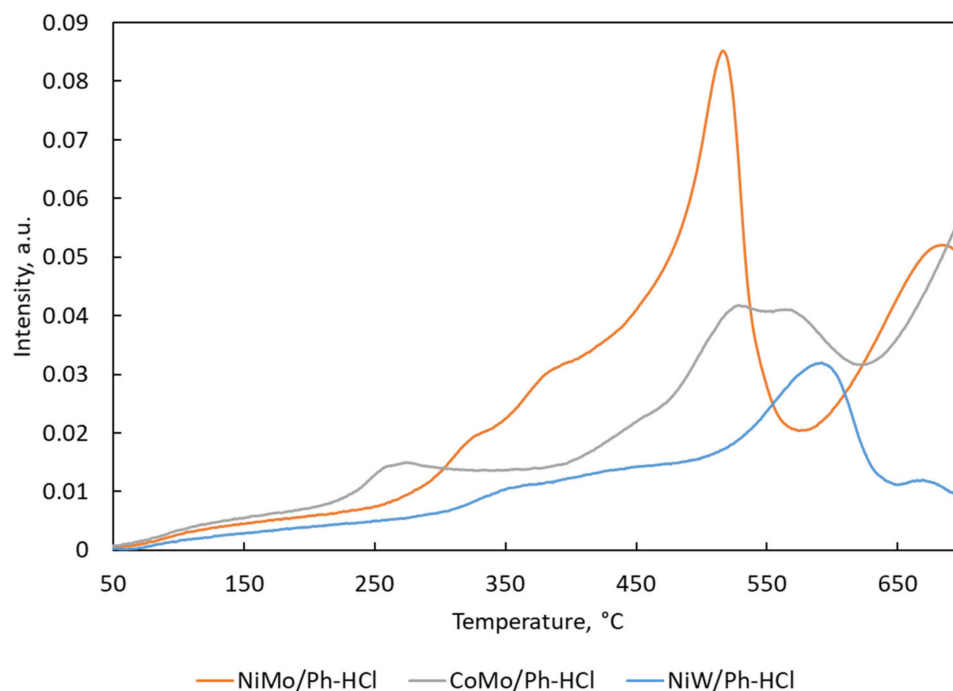


**Figure 2.** H<sub>2</sub>-TPR patterns of acid Ph-derived catalysts (NiMo/Ph-HCl, CoMo/Ph-HCl, and NiW/Ph-HCl).

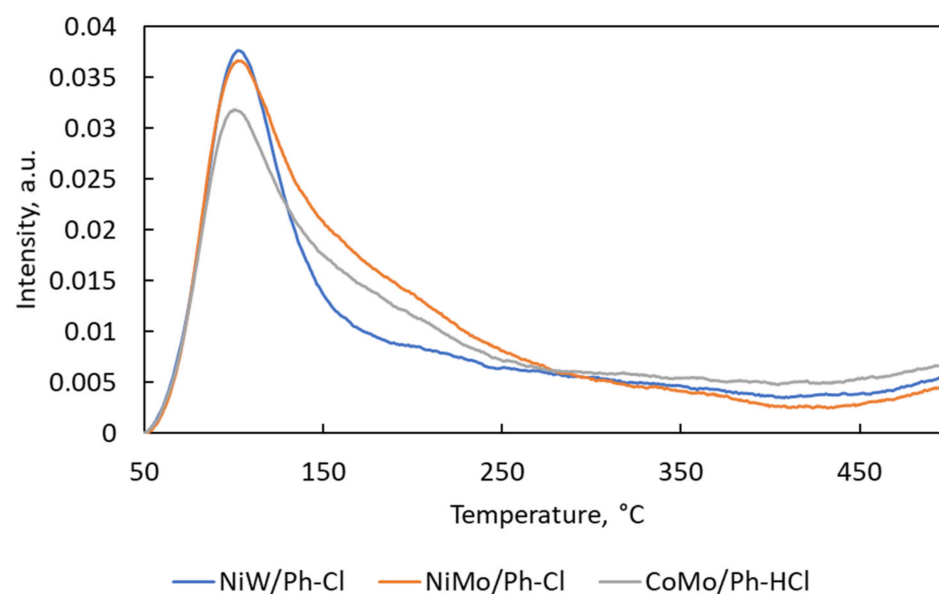


**Figure 3.** NH<sub>3</sub>-TPD profiles for all the catalysts.

CO<sub>2</sub> temperature-programmed desorption (CO<sub>2</sub>-TPD) presented the main zone of desorption peaks (50–250 °C), corresponding to the zone of weak and intermediate alkaline sites (Figure 4). The maximum of all the signals was found in the range of 105–120 °C. The most intense signal was found for NiW/Ph-HCl, indicating a higher number of weak alkaline sites. The NiMo and CoMo catalysts presented a lower number of weak sites but a relatively higher number of intermediate strong alkaline sites indicating an influence of the MoO<sub>x</sub> in increasing this type of site.

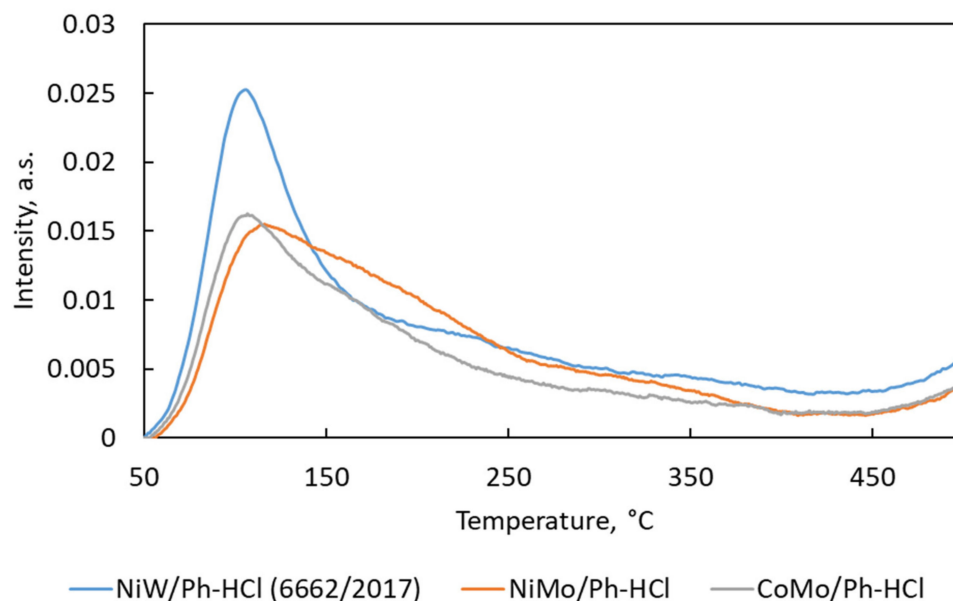


Figure 4. CO<sub>2</sub>-TPD profiles for all the catalysts.

Scanning electron microscopy (SEM) for the raw phonolite and the acid-treated phonolite are shown in Figure 5. They are in agreement with the total porosity measurements (Table 1). The acid treatment of the phonolite created a clear new type of surface. Figure 5C,D shows black holes indicating the formation of new pores during the synthesis process using the solution of HCl. The pore sizes were not homogeneous with sizes—diameters from 1–2  $\mu\text{m}$  to 5–7  $\mu\text{m}$ . So, the SEM images agree with the porosity measurement and indicate the creation of new pores of different sizes.

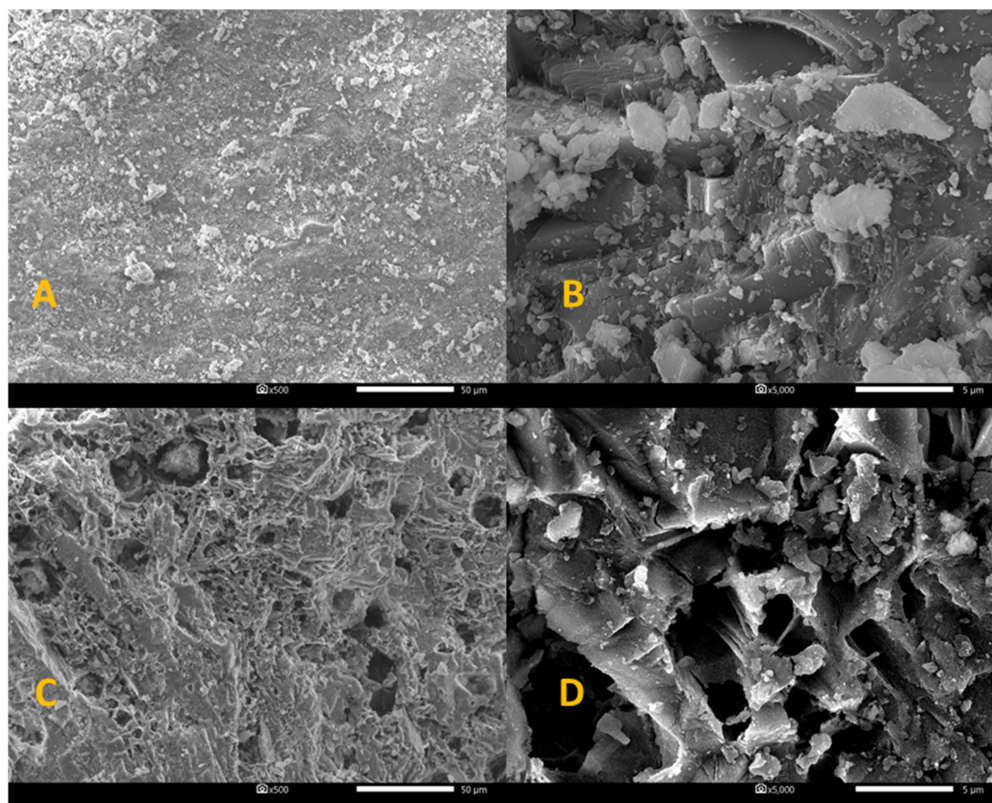
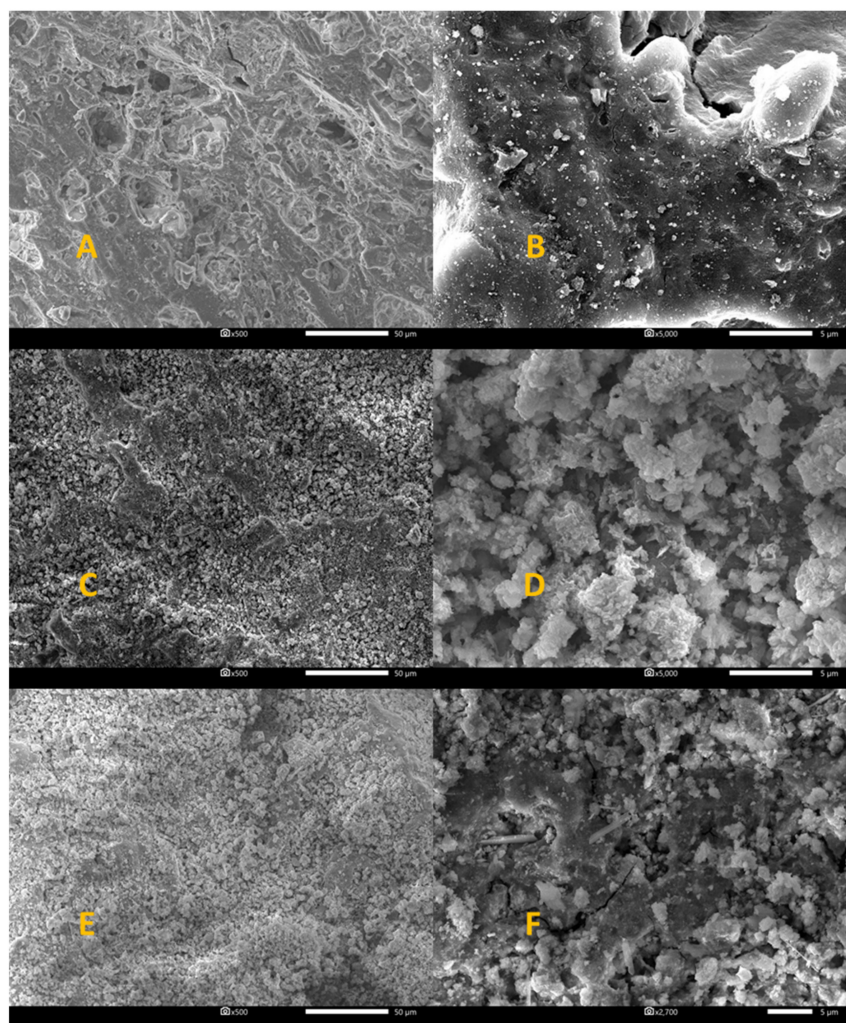


Figure 5. SEM images of the untreated phonolite (A) ( $\times 500$ ), (B) ( $\times 5000$ ) and acid-treated phonolite (C) ( $\times 500$ ), (D) ( $\times 5000$ ).

Because the raw phonolite material had very poor textural properties, an acid treatment of this raw material was performed. An increase in the total porosity and number of weak acid sites on the surface of the solid was found [14,17] resulting in an increase in the pore volume and specific surface area. These changes in the support used to produce the new catalysts are described in previous publications [14,17]. The acid treatment led to the removing of mainly Al and Na with the consequent increase of the creation of new pores in the solid.

In the case of the metal oxides supported on treated phonolite, the SEM images (Figure 6) showed that the metal oxides were filling the surface and porous, so less porous materials were obtained (Table 1). In all cases, the amorphous surface was shown in Figure 6. Electron energy dispersive X-ray spectroscopy (EDS) results are shown in Tables 2 and 3. On the surface, the HCl treatment of the Ph resulted in a decrease in the Al and Na contents. However, the Fe, Ca, and Ti contents increased (in the surface), indicating in this particular case (surface scanned) that these compounds were not on the surface in the original Ph. A high content of Mo was found for the catalysts NiMo/Ph-HCl and CoMo/Ph-HCl because of the impregnation process being the MoO<sub>x</sub> oxides present on the surface. In the case of the catalyst CoMo/Ph-HCl, a high amount of Co-O as detected on the surface indicates a high dispersion of this metal oxide instead of the W content for the catalyst NiW/Ph-HCl the W or the Ni was less dispersed. Comparing the Ni content for NiMo/Ph-HCl and NiW/Ph-HCl, the nickel content, on the surface, for NiMo catalyst was higher than for NiW catalyst.



**Figure 6.** SEM images of NiW/Ph-HCl (A) { $\times 500$ }, (B) { $\times 5000$ }), NiMo/Ph-HCl (C) { $\times 500$ }, (D) { $\times 5000$ }) and CoMo/Ph-HCl (E) { $\times 500$ }, (F) { $\times 5000$ }).

**Table 2.** EDS results. Element contents on the scanned surface (pictures at 5000× shown in Figure 5).

Phonolite (×5000)—Figure 5B			
Element	Line	Mass%	Atom%
O	K	45.91 ± 0.03	59.79 ± 0.04
Na	K	6.15 ± 0.01	5.57 ± 0.01
Al	K	11.97 ± 0.01	9.24 ± 0.01
Si	K	29.76 ± 0.02	22.08 ± 0.02
K	K	6.21 ± 0.01	3.31 ± 0.01
Acid treated phonolite (×5000)—Figure 5D			
O	K	43.74 ± 0.03	58.97 ± 0.05
Na	K	3.67 ± 0.01	3.44 ± 0.01
Al	K	7.13 ± 0.01	5.70 ± 0.01
Si	K	34.74 ± 0.03	26.68 ± 0.02
K	K	6.05 ± 0.01	3.34 ± 0.01
Ca	K	0.2 ± 0.01	0.11 ± 0.00
Ti	K	0.65 ± 0.01	0.29 ± 0.00
Fe	K	3.83 ± 0.02	1.48 ± 0.01

**Table 3.** EDS results. Element contents on the scanned surface (pictures at 5000 × shown in Figure 6).

NiW/Ph-HCl (×5000)—Figure 6B			
Element	Line	Mass%	Atom%
O	K	39.93 ± 0.03	60.51 ± 0.05
Na	K	2.12 ± 0.01	2.24 ± 0.01
Al	K	6.65 ± 0.01	5.97 ± 0.01
Si	K	26.86 ± 0.02	23.19 ± 0.02
K	K	6.34 ± 0.01	3.93 ± 0.01
Fe	K	0.38 ± 0.01	0.16 ± 0.00
Ni	K	4.87 ± 0.03	2.01 ± 0.01
Sr	L	2.01 ± 0.05	0.56 ± 0.01
W	M	10.84 ± 0.07	1.43 ± 0.01
NiMo/Ph-HCl (×5000)—Figure 6D			
O	K	31.88 ± 0.04	65.58 ± 0.08
Na	K	0.32 ± 0.01	0.46 ± 0.01
Al	K	1.57 ± 0.01	1.91 ± 0.01
Si	K	7.28 ± 0.01	8.53 ± 0.02
K	K	2.11 ± 0.01	1.78 ± 0.01
Ni	K	10.34 ± 0.04	5.80 ± 0.02
Mo	L	46.49 ± 0.05	15.95 ± 0.02

**Table 3.** *Cont.*

CoMo/Ph-HCl ( $\times 5000$ )—Figure 6F			
O	K	$36.44 \pm 0.07$	$70.68 \pm 0.14$
Na	K	$0.38 \pm 0.01$	$0.51 \pm 0.01$
Al	K	$1.37 \pm 0.01$	$1.58 \pm 0.01$
Si	K	$5.04 \pm 0.02$	$5.56 \pm 0.02$
K	K	$1.02 \pm 0.01$	$0.81 \pm 0.01$
Co	K	$13.96 \pm 0.08$	$7.35 \pm 0.04$
Mo	L	$41.80 \pm 0.08$	$13.52 \pm 0.03$

## 2.2. Catalyst Activity

MSO was reduced in a flow reactor using the three different catalysts directly, treated in a hydrogen atmosphere and with sulfided metals. Concretely the catalyst NiW/Ph-HCl results for the MSO reduction are shown in the Figure 7 (aqueous phase of the product). The main products were the MIBK, 2MP, and MPe, respectively. The sulfided NiW/Ph-HCl (NiWS<sub>x</sub>/PhHCl) catalyst was the most active solid for the MIBK and 2MP production. In the MPe production case, the catalyst reduced-activated NiW/Ph-HCl (NiW/Ph-HCl act.) was the most active one. The high content in isomesityl oxide can be due to the Bronsted acidity of the catalyst in agreement with the partial reduction of tungsten species giving extra -OH groups ( $x\text{-W=O}$  to  $x\text{-W-OH}$  change bonds) which could be responsible for the isomesityl oxide production [8]. The mesitylene production is also due to the acid sites activity, indicating that the sulfidation of the metal oxides supported on the acidified phonolite implies a decrease in the produced compounds by acid sites instead of the metal sulfides reduction activity. Thus, the activation of the catalyst at 400 °C implied an increase of Ni metal sites on the catalyst's surface, increasing the reduction of the molecules by the Ni. At 400 °C, the WO<sub>x</sub> is partially reduced, increasing the Bronsted acidity. For the catalyst sulfided NiWS<sub>x</sub>/Ph-HCl the activity was the highest for the 2MP and MIBK production.

For NiMo/Ph-HCl catalysts, the production of MIBK, 2MP, and MPe was different, where the NiMoS<sub>x</sub>/Ph-HCl catalyst was the most active in all cases for the MIBK, 2MP, and MPe production (Figure 8). The mesitylene product was produced only when the non-sulfided catalysts were used. The difference in the activity of the three catalysts is clearly explained by the time needed as the fresh catalyst is being reduced (metal oxide active sites on the surface) during the reaction, so it is the lowest active material compared to the reduced catalyst at 400 °C having the metal oxide reduced presenting a higher activity to the MIBK, 2MP, and MPe products. The sulfided NiMoS<sub>x</sub>/Ph-HCl catalyst was the most active material.

The CoMo/Ph-HCl catalyst presented a different trend (Figure 9) regarding the catalysts containing Ni and W or Mo. In the case of 2MP or MPe, the most active material was the activated catalyst at 400 °C. However, for the MIBK production, the most active material was the CoMoS<sub>x</sub>/Ph-HCl solid. This difference in the activity could be due to the high dispersion of the Co on the surface (high content of Co on the surface, as shown in Table 3), which could affect the final activity of the catalyst. The content of Mo for NiMo/Ph-HCl catalyst on the surface (Table 3) was quite lower than the CoMo/Ph-HCl catalyst indicating that a possible layer of Co is over another layer of Mo having quite higher activity when the catalyst is reduced (Table 3).

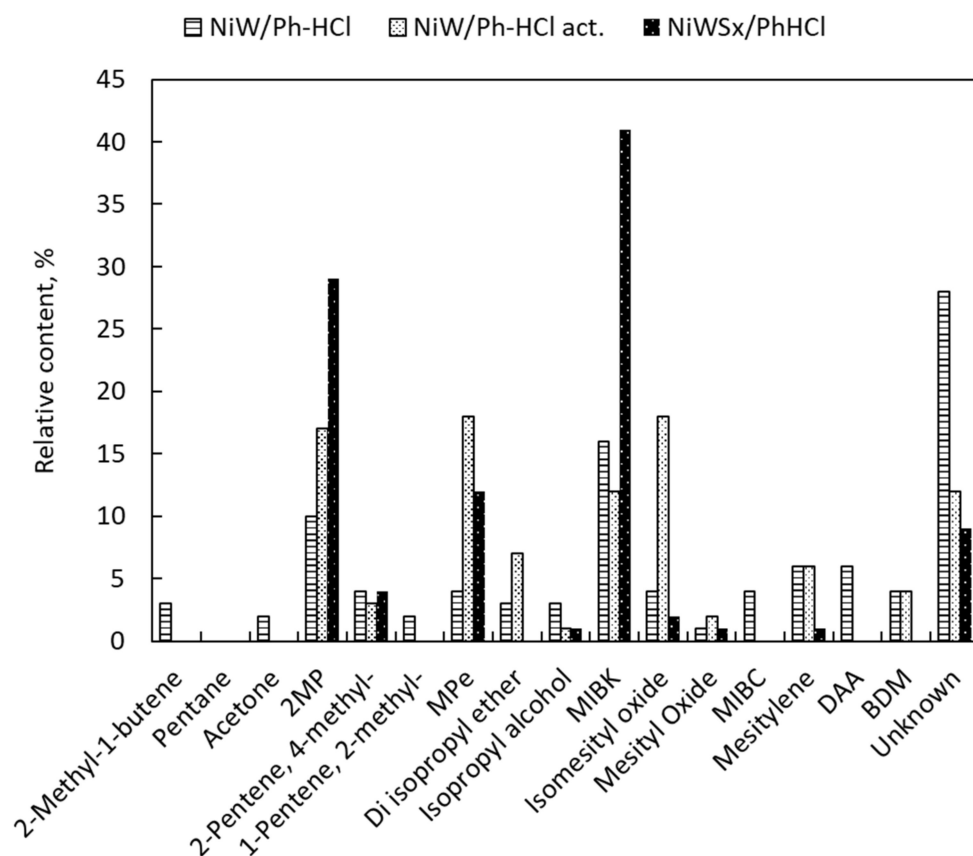


**Figure 7.** Compounds present in the organic phase of liquid product for the tests using NiW/Ph-HCl type catalysts. NiW/Ph-HCl catalyst was used directly, NiW/Ph-HCl catalyst was previously reduced in hydrogen atmosphere and NiWSx/Ph-HCl material was previously treated for the sulfidation of the metal oxides. BDM abbreviation refers to benzene, 1,4-dimethyl-2-(2-methylpropyl)-.

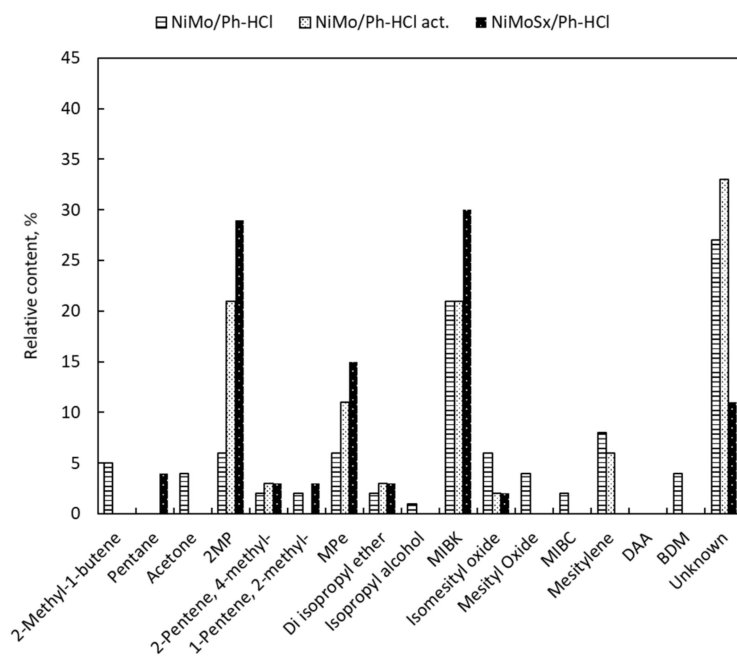


**Figure 8.** Compounds present in the organic liquid product for the tests using NiMo/Ph-HCl type catalysts. NiMo/Ph-HCl catalyst was used directly, NiMo/Ph-HCl catalyst was previously reduced in hydrogen atmosphere and NiMoSx/Ph-HCl material was previously treated for the sulfidation of the metal oxides.

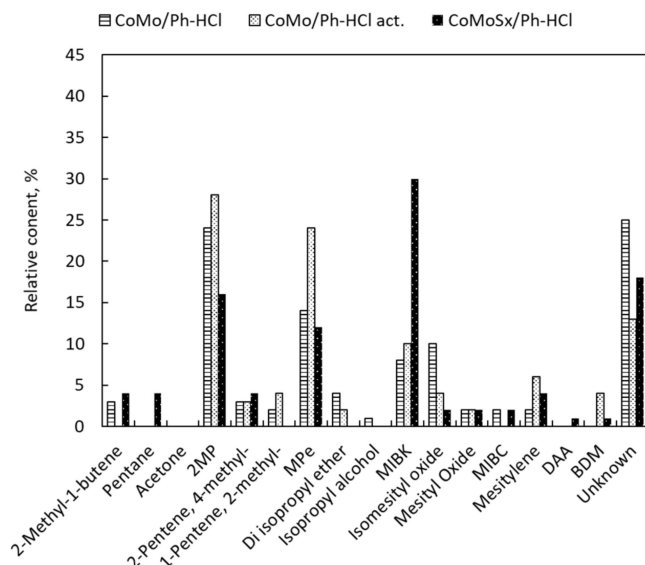


**Figure 9.** Compounds present in the organic liquid product for the tests using CoMo/Ph-HCl type catalysts. CoMo/Ph-HCl catalyst was used directly, CoMo/Ph-HCl catalyst was previously reduced in hydrogen atmosphere and CoMoSx/Ph-HCl material was previously treated for the sulfidation of the metal oxides.

In all cases, the reactions produced gas, liquids, and solids (Figure 10). In the case of the liquids, they were classified in water-soluble liquids and organic soluble liquids. The water-soluble liquid presented a similar attenuated total reflectance-Fourier transform infrared (ATR-FTIR) to the pure demineralized water. The water-soluble liquids could be a mixture of water and polar compounds (alcohols, ketones). The deoxygenation of the MSO produces water with other non-known compounds. For this work, only the liquids non-soluble in water were analyzed. The test using NiMo/Ph-HCl act. was the only test producing a high amount of aqueous liquid over 20 wt% producing at the same time the highest content of gases (Figure 10). For the other catalytic tests using NiW/Ph-HCl or CoMo/Ph-HCl, the aqueous phase content was similar. The gases (gaseous phase at room temperature) content decreased with the activation and sulfidation of the NiW/Ph-HCl catalyst, and the organic phase content increased. In the CoMo/Ph-HCl catalyst, the amount of organic (non-water-soluble) liquids decreased with the CoMo/Ph-HCl catalyst but increased with the CoMoSx/Ph-HCl solid. In all cases, the highest yield of organic liquids was found for the sulfided metal catalysts.

The yields to MIBK, 2MP, and MPe are represented in Figure 11. The main products in all cases were the MIBK and 2MP. The catalysts having metal sulfided active sites were the most active for the MIBK production and the deoxygenation to 2MP. The MPe formation was independent of the MIBK or 2MP production. The decrease in the yield to 2MP or MIBK for the tests using the activated catalysts in H<sub>2</sub> could be due to the formation of Bronsted acidity for the partially reduced metals. The most active catalyst for the MIBK production was the NiWSx/Ph-HCl. For the 2MP production, the catalyst NiMoSx/Ph-HCl (similar 2MP production as for catalyst NiWSx/Ph-HCl) was the most active solid. In the case of MPe, its production trend was not clear, decreasing for NiMo and CoMo type catalysts but having a different trend for the NiW type catalyst, increasing its product amount for the NiW/Ph-HCl act. regarding the NiW/Ph-HCl.

The results from literature are difficult to compare to the results obtained in this work because of the use of different types of catalysts, reaction conditions (temperature, pressure, MSO pure or in a solvent). Concretely the yield of MIBK was 99 wt% [10] by using a Pd/SiO<sub>2</sub> catalyst or membrane commercial Pd-doped Amberlyst catalyst [9] with 35 wt% of MSO content in the product but starting with acetone as the raw material. Pt noble metal used in other previous work [11] led to a high yield to 2MP compared to the results

obtained in this work. In summary, if we compare our results with the literature [8–11] we obtained lower yields to MIBK or 2MP separately. However, the reactions performed in this research work led to the production of MIBK and 2MP together. According to our previous work, it is possible to increase the MIBK production or 2MP regarding the feed flow [16]. In addition, as written previously, the catalysts used in this case were noble metals but sulfide metals were supported on phonolite with different experimental conditions. Regarding to sulfide metal catalysts, no results were found in literature to compare these yields.

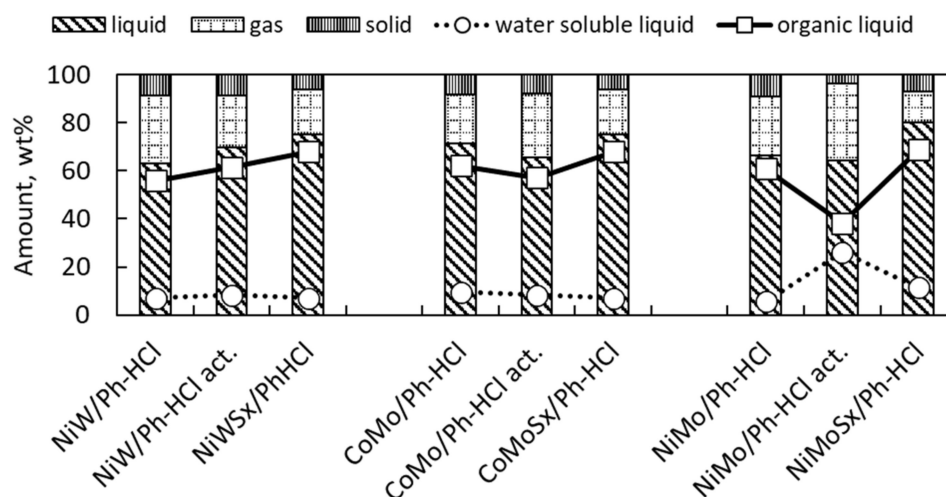


Figure 10. Gas-solid-liquid mass balance for all the catalytic tests.

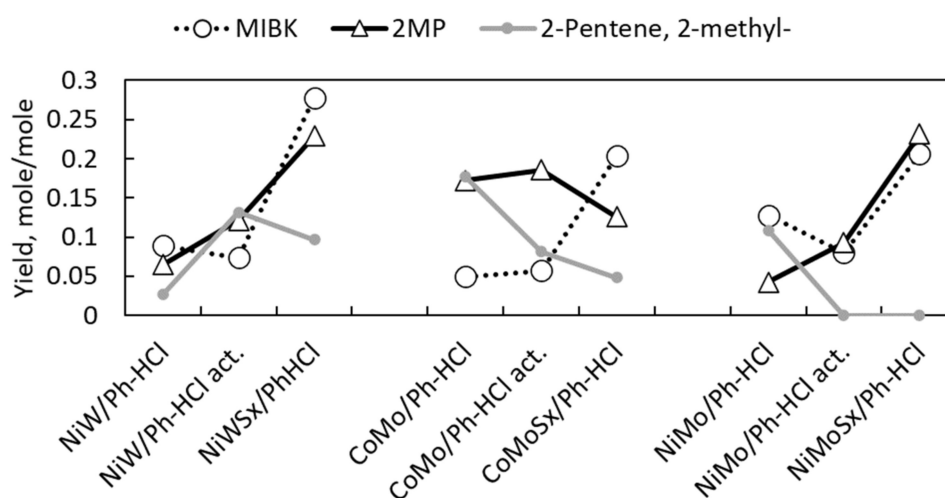


Figure 11. Yield of MIBK, 2MP, and MPE. The yield was calculated by the division of the moles produced of each compound and the initial amount of moles of MSO.

Figure 12 shows a proposal summary about the production of the main products MIBK, 2MP and the other secondary products. The reactions of decarboxylation and decarbonylation were not included. However, for the production of MIBK, 2MP, and MPE, this scheme could clarify the steps of the production of these molecules.

For the gases production (Figure 13), the test using catalysts NiW/Ph-HCl presented the highest amount of CO + CO<sub>2</sub> products. In addition, CO + CO<sub>2</sub> was the main product because of the production of products with less content in oxygen. The contents of propane and propylene were high for the catalyst without activation and were activated in pure hydrogen. This tendency was found higher for catalysts CoMo/Ph-HCl and NiMo/Ph-HCl. C<sub>4</sub> compounds were also produced as a consequence of the cracking reactions. Concretely, isobutane and isobutene were produced.

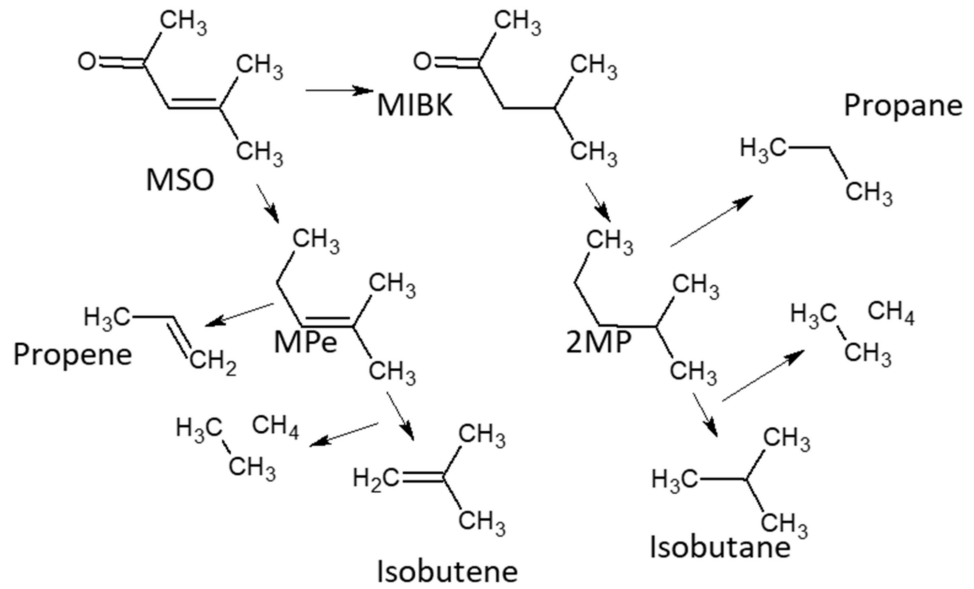


Figure 12. Proposed reaction scheme for the production of MIBK, 2MP, MPe, propene, propane, isobutene, and isobutane.

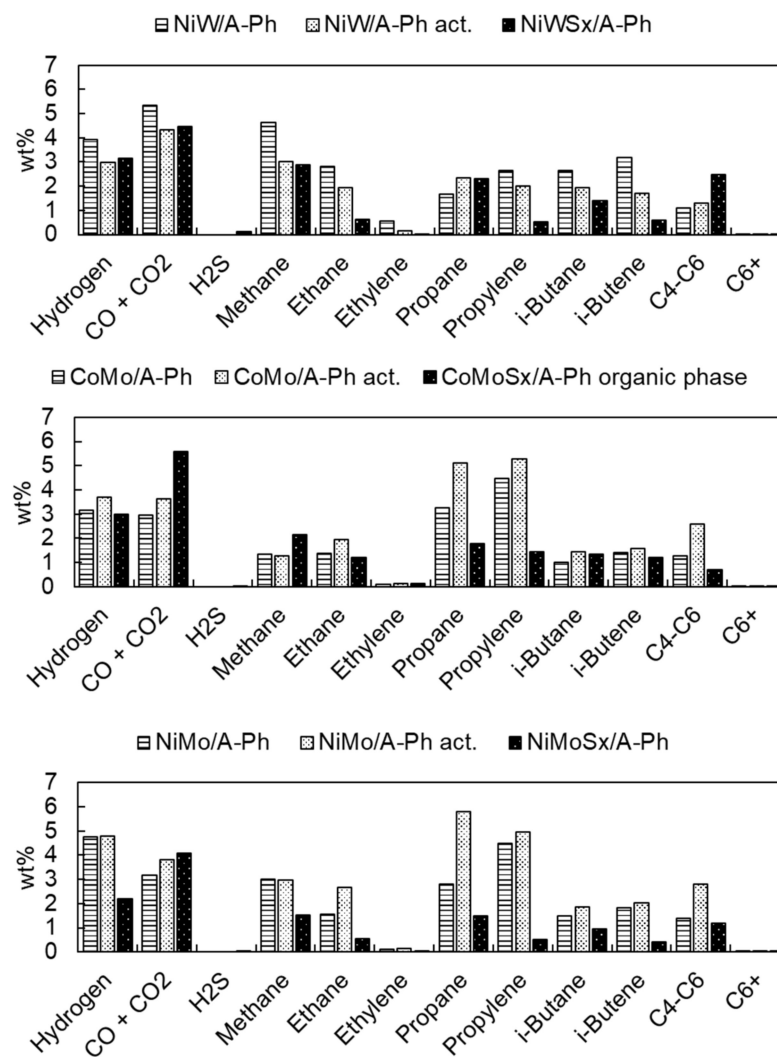


Figure 13. Refinery gas analyses (RGA) results for gases.

### 3. Materials and Methods

#### 3.1. Raw Materials

Ammonium molybdenate tetrahydrate  $(\text{NH}_4)_6\text{Mo}_7\text{O}_{24}\cdot 4\text{H}_2\text{O}$  G.R. 99%, cobalt nitrate hexahydrate  $(\text{Co}(\text{NO}_3)_2\cdot 6\text{H}_2\text{O}$  G.R. 99% from the company Lach-ner s.r.o., nickel nitrate hexahydrate  $(\text{NiNO}_3)\cdot 6\text{H}_2\text{O}$  purum p.a., crystallized,  $\geq 97.0\%$  and ammonium metatungstate hydrate  $(\text{NH}_4)_6\text{H}_2\text{W}_{12}\text{O}_{40}\cdot x\text{H}_2\text{O}$  99.99% from the company Sigma Aldrich were used for the catalyst synthesis.

The Ph was supplied by the company KERAMOST a.s. (Most, Czechia) and the ore source was located in the Northwest of Czech Republic.

The MSO (98%) was synthesized by the Research Institute ORLEN UniCRE a.s. by a previous aldol condensation standard catalytic reaction of acetone. Aldol condensation of acetone to form diacetone alcohol (DAA) was performed by using Mg-Al hydrotalcite with molar ratio of Mg:Al 2:1 ( $2\times$  Acetone  $\Leftrightarrow$   $1\times$  DAA). Then, DAA was dehydrated by using a  $\text{H}_3\text{PO}_4/\text{Al}_2\text{O}_3$  catalyst. The final purification of MSO to obtain a MSO 98 wt% was obtained by distillation removing residues of acetone, DAA, and other products. No more details are given because of the different aim of this publication and the possibility of buying this raw material from other commercial companies.

#### 3.2. Catalysts Synthesis and Characterization

The raw material was treated according to literature [17]. The catalyst support was synthesized using a Ph which was treated with hydrochloric acid (the Ph was supplied in sand form with a size of 0–2 mm). The Ph acidly treated was called Ph-HCl. Before the catalyst preparation, the Ph sand was sieved using a Retsch AS300. Twenty grams of Ph (224–560 mm fraction) was used. Then, it was dried at 120 °C overnight and was leached using a 3 M HCl demineralized water solution. The mixture was stirred at 80 °C for 4 h having a Ph/acid (g/mL) ratio of 1:10 wt/vol. The product was then filtered, washed (with hot demineralized water), and dried overnight at 120 °C. The dried solids were calcined at 500 °C for 6 h ( $1\text{ }^\circ\text{C min}^{-1}$  at room temperature) in air. Then, the nickel, cobalt, molybdenum, or tungsten sources were used to synthesize each catalyst. The resulting solids (Ph-HCl support) were impregnated with each metal oxide source. Finally, the catalyst precursors were calcined for 6 h at 450 °C ( $1\text{ }^\circ\text{C min}^{-1}$ ) in air. Three catalysts containing nickel-tungsten (NiW), cobalt-molybdenum (CoMo), and nickel-molybdenum (NiMo) were created: NiW/Ph-HCl, CoMo/Ph-HCl, and NiMo/Ph-HCl respectively.

The composition of the catalysts was ascertained by XRF using an S8 Tiger (Bruker AXS, Advanced X-ray Solutions GmbH, Karlsruhe, Germany) with an Rh cathode. The crystallographic structures of the catalysts were determined by examining the XRD patterns of the powder samples obtained via a D8 Advance ECO (Bruker) applying Cu K  $\alpha$  radiation ( $\lambda = 1.5406\text{ \AA}$ ). A step size of  $0.02^\circ$  and a step time of 0.5 s were used. For catalysts containing Mo, the elemental analysis was carried out by the ICP method using ICP-EOS Agilent 725 (Agilent Technologies Inc., Santa Clara, CA, USA).

The acidic properties of the catalysts were characterized by  $\text{NH}_3$ -TPD temperature-programmed desorption using an Autochem 2950 HP (Micromeritics Instrument Corporation, Norcross, GA, USA). In a quartz U-tube reactor, a total of 100 mg of the sample was pre-treated in He to 450 °C, with a temperature ramp rate of  $10\text{ }^\circ\text{C min}^{-1}$ . The sample was then cooled to 50 °C and saturated with ammonia at a flow rate of  $25\text{ mL min}^{-1}$  of 10 vol%  $\text{NH}_3/\text{He}$  for 30 min. The gas was subsequently changed to helium ( $25\text{ mL/min}$ ) and flushed out until the baseline was continuous (60 min). After this procedure, the temperature increased to 500 °C at a rate of  $15\text{ }^\circ\text{C min}^{-1}$  to obtain the  $\text{NH}_3$ -TPD curves from 100 to 500 °C, with a ramp rate of  $15\text{ }^\circ\text{C min}^{-1}$ . The changes in gas concentration were monitored by a TCD detector. The  $\text{CO}_2$ -TPD analyses were realized using the same procedure for  $\text{NH}_3$ -TPD. They were performed to characterize the alkaline properties of the catalysts.

The specific surface area BET for the catalysts was determined by  $\text{N}_2$  adsorption/desorption at  $-196\text{ }^\circ\text{C}$  (Autosorb iQ). Mercury porosimetry measurements were performed on a Mi-

comeritics AutoPore IV 9510 mercury porosimeter (Micromeritics Instrument Corporation, Norcross, GA, USA). All samples were dried (before the analysis for specific surface area BET and mercury porosimetry measurements) in a glass-cell at 200 °C under vacuum for 16 h.

Morphology of the samples was studied by a scanning electron microscope JSM-IT500HR from JEOL (JEOL, Tokyo, Japan). The voltage was 15 kV and the detector used was secondary electron (SED). The working distance was 10 mm and magnification range was from 150× to 10,000×. Mapping analysis was performed using an EDS probe. Samples were coated with about 5 nm of gold, to make them conductive and to prevent charging of the samples in the microscope.

### 3.3. Experimental Set up and Catalytic Tests

An autoclave 4575/76 with a “4848B” controller (Parr Instruments Company, Moline, IL, USA) was used for all tests. Three types of reactions were carried out: (i) with sulfided metal-supported catalysts, (ii) reduced in H<sub>2</sub> metal-supported catalysts and, (iii) using the catalysts directly without any activation.

- i. For the activation by the active metal sulfidation, the metal oxide-supported catalysts were activated—sulfided using di-*t*-butyl polysulfide (Lubrizol Company, Wickliffe, OH, USA). In total, 2.1 g of the catalyst and 10 g of di-*t*-butyl polysulfide were introduced into the reactor. The reactor was pressurized to 50 bar and heated from room temperature to 375 °C (8.3 °C min<sup>-1</sup>) while maintaining the temperature for 1 h. The reactor was then cooled to room temperature and depressurized.
- ii. For the activation by the metal reduction only under H<sub>2</sub> atmosphere, the autoclave was pressurized to 50 bar and heated from room temperature to 400 °C (8.3 °C min<sup>-1</sup>). The temperature of 400 °C was maintained for 2 h. Then, the reactor was cooled to room temperature and depressurized. About 2.1 g of catalyst (metal oxide) was used for this case.
- iii. For the direct use of the catalyst, 2.1 g of fresh catalyst was directly introduced in the batch reactor to start the reaction.

A total of nine reactions for the MSO reduction were carried out because three starting solids (NiW/Ph-HCl, NiMo/Ph-HCl, and CoMo/Ph-HCl) were used. For the MSO reduction tests, the resulting activated catalyst from using 2.1 g of initial solid or directly 2.1 g of catalyst (without any activation) were used. Then, for each reaction, 25 g of MSO was added, the autoclave with catalyst and MSO was then flushed with nitrogen to avoid air contamination and then pressurized at 100 bar in nitrogen (pressure test security-safety) for 1 h. After that, the autoclave was depressurized and flushed with H<sub>2</sub> at 1 bar and then pressurized to 50 bar (H<sub>2</sub>) at room temperature. The autoclave was then heated to 375 °C (8.3 °C min<sup>-1</sup>), maintaining this temperature for 1 h. The autoclave was then cooled by airflow up to 30 °C to collect the gaseous sample. Then, the autoclave was cooled to room temperature, opened and weighed to obtain the mass balance (subtracting the final and initial autoclave filled weights). The liquid was then collected, weighed, centrifuged, and filtered (cold filtration).

### 3.4. Product Analyses

The mass balance was calculated by weighting the total filtrated sediment and liquids (cold filtration). Liquid products were centrifuged in 40 mL vials at 2600 rpm for 30 min, thereby obtaining a clean liquid as the supernatant, with solids + non-miscible liquid mixtures at the bottom. The initial catalyst amount was subtracted from the total amount of solids to calculate the solid product amounts.

The gas composition was characterized by Agilent’s Refinery Gas Analyzer (RGA) method (Agilent, Santa Clara, CA, USA). The organic liquid samples were analyzed using a GC/MS QP2010 Shimadzu GC-2010 Plus with a chromatographic column RTX-5. Oven temperature: (1) 35 °C for 0.17 h, (2) 35 to 100 °C (5 °C/min), (3) 100–320 °C (10 °C/min), (4) 320 °C for 0.17 h; carrier gas: He. Water-soluble and solid samples were not analyzed. MSO,

MIBK, 2MP, and MPe contents in the products were calculated according to a previous calibration carried out in a GC-FID.

#### 4. Conclusions

The phonolite catalysts were active in the MSO reduction. Three materials based in acid-treated phonolite as support were used and tested for the MSO reaction to MIBK and 2MP. These materials were used directly or activated in hydrogen or sulfided having a total of nine catalysts which were tested for the MSO reduction. MSO reacted mainly to MIBK and 2MP and also to other secondary compounds. A maximum yield of 30% to MIBK was found for the catalyst NiWSx/Ph-HCl. Sulfided metal supported catalysts were the most active solids for the MIBK production. The fresh catalysts, activated in hydrogen catalysts, and sulfided metal-supported activity differences were mainly found in the MIBK production. The MIBK production, in general, was increasing in agreement with the order: fresh catalyst > H<sub>2</sub> activated catalyst > sulfided metal supported catalyst. For NiW/Ph-HCl catalysts, the 2MP production was increasing progressively in the order of NiW/Ph-HCl > NiW/Ph-HCl act. > NiWSx/Ph-HCl. However, for the catalysts NiMo/Ph-HCl and CoMo/Ph-HCl, it did not present any clear trend, showing only less production of 2MP for the fresh catalysts.

**Author Contributions:** Conceptualization, J.M.H.H., Z.T. and J.K.; methodology, J.M.H.H., J.K., J.F. and R.V.; validation, J.M.H.H. and H.d.P.C.; formal analysis, Z.T., R.V., I.H. and J.F.; investigation, J.M.H.H. and J.F.; resources, J.M.H.H.; data curation, J.M.H.H. and Z.T.; writing—original draft preparation, J.M.H.H.; writing—review and editing, H.d.P.C., J.M.H.H., Z.T. and J.K.; visualization, J.M.H.H.; supervision, H.d.P.C., Z.T. and J.M.H.H.; project administration, J.M.H.H. All authors have read and agreed to the published version of the manuscript.

**Funding:** The publication is a result of the project which was carried out within the financial support of the Ministry of Industry and Trade of the Czech Republic with institutional support for long-term conceptual development of research organization. The result was achieved using the infrastructure included in the project Efficient Use of Energy Resources Using Catalytic Processes (LM2018119) which has been financially supported by MEYS within the targeted support of large infrastructures.

**Conflicts of Interest:** The authors declare no conflict of interest.

#### References

1. Salvapati, G.S.; Ramanamurty, K.V.; Janardanarao, M. Selective catalytic self-condensation of acetone. *J. Mol. Catal.* **1989**, *54*, 9–30. [[CrossRef](#)]
2. Mesityl Oxide. Hazardous Substance Fact Sheet. New Jersey Department of Health and Senior Services. Occupational Health Service. Trenton, NJ 08625-0360, June 1999. Available online: <https://nj.gov/health/eoh/rtkweb/documents/fs/1195.pdf> (accessed on 6 September 2021).
3. Kuśtrowski, P.; Sułkowska, D.; Chmielarz, L.; Rafalska-Łasocha, A.; Dudek, B.; Dziembaj, R. Influence of thermal treatment conditions on the activity of hydrotalcite-derived Mg–Al oxides in the aldol condensation of acetone. *Microporous Mesoporous Mater.* **2005**, *78*, 11–22. [[CrossRef](#)]
4. Thotla, S.; Agarwal, V.; Mahajani, S.M. Simultaneous production of diacetone alcohol and mesityl oxide from acetone using reactive distillation. *Chem. Eng. Sci.* **2007**, *62*, 18–20. [[CrossRef](#)]
5. Tan, S.T.; Ali Umar, A.A.; Salleh, M.M. Synthesis of defect-rich, (001) faceted-ZnO nanorod on a FTO substrate as efficient photocatalysts for dehydrogenation of isopropanol to acetone. *J. Phys. Chem. Solids* **2016**, *93*, 73–78. [[CrossRef](#)]
6. Hauser, M. The reactions of mesityl oxide. *Chem. Rev.* **1963**, *63*, 311–324. [[CrossRef](#)]
7. Wisniak, J.; Herskowitz, M.; Roffe, D.; Smllovitz, S. Reduction of Mesityl Oxide. *Ind. Eng. Chem. Prod. Res. Dev.* **1976**, *15*, 163–168. [[CrossRef](#)]
8. O’Keefe, W.K.; Jiang, M.; Ng, F.T.T.; Rempel, G.L. Liquid phase kinetics for the selective hydrogenation of mesityl oxide to methyl isobutyl ketone in acetone over a Pd/Al<sub>2</sub>O<sub>3</sub> catalyst. *Chem. Eng. Sci.* **2005**, *60*, 4131–4140. [[CrossRef](#)]
9. Nicol, W.; du Toit, E.L. One-step methyl isobutyl ketone synthesis from acetone and hydrogen using Amberlyst®CH28. *Chem. Eng. Process. Process. Intensif.* **2004**, *43*, 1539–1545. [[CrossRef](#)]
10. Ho, C.R.; Zheng, S.; Shylesh, S.; Bell, A.T. The mechanism and kinetics of methyl isobutyl ketone synthesis from acetone over ion-exchanged hydroxyapatite. *J. Catal.* **2018**, *365*, 174–183. [[CrossRef](#)]
11. Alotaibi, M.A.; Kozhevnikova, E.F.; Kozhevnikov, I.V. Hydrogenation of methyl isobutyl ketone over bifunctional Pt–zeolite catalyst. *J. Catal.* **2012**, *293*, 141–144. [[CrossRef](#)]

12. Weisser, O.; Landa, S. Sulphide Catalysts, Their Properties and Applications. Institute of Chemical Technology, Prague. *ACADEMIA Publ. House Czechoslov. Acad. Sci.* **1972**, *6.6.1.*, 168–171.
13. Hidalgo-Herrador, J.M.; Fratzczak, J.; Velvarská, R.; de Paz Carmona, H. Oxalic acid-mediated catalytic transfer hydrodeoxygenation of waste cooking oil. *Mol. Catal.* **2020**, *491*, 110973. [[CrossRef](#)]
14. Hidalgo Herrador, J.M.; Fratzczak, J.; Tišler, Z.; de Paz Carmona, H.; Velvarská, R. Oxalic Acid as a Hydrogen Donor for the Hydrodesulfurization of Gas Oil and Deoxygenation of Rapeseed Oil Using Phonolite-Based Catalysts. *Molecules* **2020**, *25*, 3732. [[CrossRef](#)]
15. Hidalgo, J.M.; Tišler, Z.; Vráblík, A.; Velvarská, R.; Lederer, J. Acid-modified phonolite and foamed zeolite as supports for NiW catalysts for deoxygenation of waste rendering fat. *Reac. Kinet. Mech. Cat.* **2019**, *126*, 773–793. [[CrossRef](#)]
16. Hidalgo Herrador, J.M.; Fratzczak, J.; Tišler, Z.; Velvarská, R.; Kocík, J. Nickel-Tungsten Catalyst Based on Oxalic Acid Modified Phonolite. UTILITY MODEL. Group UM App. No. 2021-38717. Document No. CZ 35055 U1. Industrial Property Office of the Czech Republic. Available online: [https://isdv.upv.cz/webapp/resdb.print\\_detail.det?pspis=PUV/38717&plang=EN](https://isdv.upv.cz/webapp/resdb.print_detail.det?pspis=PUV/38717&plang=EN) (accessed on 10 September 2021).
17. Hidalgo-Herrador, J.M.; Tišler, Z.; Hajková, P.; Soukupová, L.; Zárbynická, L.; Černá, K. Cold Plasma and Acid Treatment Modification Effects on Phonolite. *Acta Chim. Slov.* **2017**, *64*, 598–602. [[CrossRef](#)]
18. de Paz Carmona, H.; Hidalgo Herrador, J.M.; Fratzczak, J.; Tišler, Z. Nickel-Molybdenum Catalyst on an Acid-Modified Unit. UTILITY MODEL. Group UM App. No. 2020-38225. Document No. CZ CZ 34683 U1. Industrial Property Office of the Czech Republic. Available online: [https://isdv.upv.cz/webapp/resdb.print\\_detail.det?pspis=PUV/38225&plang=CS](https://isdv.upv.cz/webapp/resdb.print_detail.det?pspis=PUV/38225&plang=CS) (accessed on 10 September 2021).
19. Henderson, C.M.B. Composition, Thermal Expansion and Phase Transitions in Framework Silicates: Revisitation and Review of Natural and Synthetic Analogues of Nepheline-, Feldspar- and Leucite-Mineral Groups. *Solids* **2021**, *2*, 1. [[CrossRef](#)]
20. Long, H.; Shi, T.; Hu, H.; Jiang, S.; Xi, S.; Tang, Z. Growth of Hierarchical Mesoporous NiO Nanosheets on Carbon Cloth as Binder-free Anodes for High-performance Flexible Lithium-ion Batteries. *Sci. Rep.* **2014**, *4*, 7413. [[CrossRef](#)] [[PubMed](#)]
21. Wang, X.G.; Yang, N.H.; Yuan, L.; Pang, S.J. High-resolution electron microscopy analysis of microstructural changes in WO<sub>x</sub> electrochromic films. *Surf. Coat. Technol.* **1998**, *110*, 184–187. [[CrossRef](#)]
22. Bulavchenko, O.A.; Cherepanova, S.V.; Malakhov, V.V.; Dovlitova, L.S.; Ishchenko, A.V.; Tsybulya, S.V. In situ XRD study of nanocrystalline cobalt oxide reduction. *Kinet. Catal.* **2009**, *50*, 192–198. [[CrossRef](#)]
23. Zhang, Z.; Wang, Q.; Chen, H.; Zhang, X. Hydroconversion of Waste Cooking Oil into Green Biofuel over Hierarchical USY-Supported NiMo Catalyst: A Comparative Study of Desilication and Dealumination. *Catalysts* **2017**, *7*, 281. [[CrossRef](#)]
24. Gnanamani, M.K.; Jacobs, G.; Graham, U.M.; Pendyala, V.R.R.; Martinelli, M.; MacLennan, A.; Hu, Y.; Davis, B.H. Effect of sequence of P and Co addition over silica for Fischer-Tropsch synthesis. *Appl. Catal. A-Gen.* **2017**, *538*, 190–198. [[CrossRef](#)]